

The Readiness of Water Molecules to Split into Hydrogen + Oxygen: A Proposed New Aspect of Water Splitting

Helmut Schäfer,* Anja Schuster, Stefan Kunis, Tom Bookholt, Jörg Hardege, Klara Rüwe, and Julia Brune

The potential of the anode, at which the evolution of oxygen begins, is a key parameter that describes how well water is split in water electrolyzers. Research efforts related to electrocatalytically initiated water splitting that aim at reducing the oxygen evolution reaction (OER) overpotential to date focus on the optimization of materials used to produce the electrodes. Descriptors for the readiness of the H₂O molecule itself to break down into its components have not been considered in water electrolysis experiments so far. In a simple set of experiments, it is found that adding dioxane to aqueous solutions leads to a substantial blueshift of the frequency of the O–H stretch vibration which is a sign of an increased strength of the O–H bond (intramolecular bonding). This phenomenon coincides with a significant increase in the OER onset potential as derived from cyclic voltammetry experiments. Thus, the O–H stretch frequency can be an ideal indicator for the readiness of water molecules to be split in its cleavage products. This is thought to be first example of a study into the relationship between structural features of water as derived from Fourier transform infrared (FTIR) spectroscopic studies and key results derived from water electrolysis experiments.

1. Introduction

Electrocatalytically initiated water splitting when powered by the sun represents a CO₂ footprint-free access to the energy carrier of the future, hydrogen. The competitiveness of water electrolysis however stands and falls with the cell voltage required to achieve reasonable current densities and thus material turnover. Although for industrial use hydrogen is the cleavage product that matters in water splitting, the oxygen evolution reaction (OER) also plays a key role since most of the total overvoltage added to the cell voltage occurs on the anode side. The potential of the anode at which the evolution of oxygen begins, and the anode potential at which a certain current density is ensured, are significant parameters that describe how well the water splitting takes place. The influence of electrocatalysts on these parameters has subsequently been discussed particularly intensively in the last decades.^[1–4]

A conservative estimate is that ≈80 000 scientific articles are directly or indirectly related to improving electrodes (electrocatalysts) with the aim of making OER more efficient. To our knowledge, descriptors for the readiness of the H₂O molecules to break down into hydrogen and oxygen have not been considered in water electrolysis optimization experiments so far.

Vibrational spectroscopy is known to be a powerful tool for studying the microscopic structure of water, that is, the structure on a molecular level as well as the cooperative hydrogen-bond network.^[5,6] Thus, infrared spectroscopy is suitable to investigate both the intermolecular- and the intramolecular structure of water which is crucial for its fundamental physical properties, its role in natural processes and its behavior in chemical reactions.^[7,8] Investigations are based on the O–H stretch mode^[5,9,10] and the H–O–H bending mode.^[11] Liquid water has a wide range of H-bond angles and distances, and the distribution of H-bond configurations leads to a (broad) distribution of O–H stretch frequencies, that is, to a large spectral breadth. This gives a good basis for the overlap of the O–H stretch band with other vibrational bands in more complex systems as it leads to a complex interplay of intramolecular intermode and intermolecular intramode couplings. In contrast to the O–H stretching mode, the H–O–H bending mode is unique to the H₂O molecule; it

H. Schäfer, T. Bookholt, K. Rüwe, J. Brune
University of Osnabrück
The Electrochemical Energy and Catalysis Group
Barbarastrasse 7, 49076 Osnabrück, Germany
E-mail: helmut.schaefer@uos.de

A. Schuster
University of Osnabrück
Institute of Chemistry
Inorganic Chemistry II
Barbarastrasse 7, 49076 Osnabrück, Germany

S. Kunis
Institute of Mathematics and Center for Cellular Nanoanalytics
Osnabrück University
49076 Osnabrück, Germany

J. Hardege
University of Hull
School of Natural Sciences
Hull University
Hull HU67RX, UK

 The ORCID identification number(s) for the author(s) of this article can be found under <https://doi.org/10.1002/adma.202300099>

© 2023 The Authors. Advanced Materials published by Wiley-VCH GmbH. This is an open access article under the terms of the Creative Commons Attribution License, which permits use, distribution and reproduction in any medium, provided the original work is properly cited.

DOI: 10.1002/adma.202300099

has only one H–O–H fragment and, hence there cannot be intramolecular vibrational coupling between two bending modes.

There are two main reasons why we have focused principally on the O–H stretch mode despite these obvious disadvantages:

- i. The OH stretching frequency is an excellent probe of local H-bond alignment; in contrast to the bending mode, which is a direct probe of the hydrogen network. Therefore, the investigation of the stretching mode is better suited to the electrolytes used in common water electrolysis cells.
- ii. The thermodynamic (equilibrium) decomposition voltage (E_0) of water is mathematically related to the Gibbs free enthalpy (ΔG_0) of the water splitting reaction, and as such refers to $\Delta G_0 = -zFE_0$ where z is the number of electrons converted per formula unit and F is the Faraday constant. The Gibbs free enthalpy in turn is based on the O–H bond strength in a water molecule (intramolecular bonding). In other words, the equilibrium cell voltage depends inter alia on the O–H bond strength (intramolecular bonding).

The equilibrium cell voltage in turn is given by both half-cell potentials, the equilibrium potential that can be assigned to the oxygen evolution- and the corresponding potential that can be assigned to the hydrogen evolution reaction. The connection between the strength of the O–H bond in a water molecule and the potential at which oxygen evolution begins therefore not only seems logical; on the contrary, one can derive a causal relationship between the two quantities on the basis of physical-mathematical relationships.

In addition, there is a known (negative) correlation between the frequency of the O–H stretch vibration and the hydrogen bond strength (bond strength between H-bonded molecules;^[10] intermolecular bonding):

The vibrational frequency is inversely related to the hydrogen bond strength also defined as donor–acceptor interaction of water pairs or two-body delocalization-energy $\Delta E_{D \rightarrow A}$.^[12,13]

$$\Delta E_{D \rightarrow A} \text{ (kJ mol}^{-1}\text{)} = 0.0392 - 150.6 \omega \text{ (cm}^{-1}\text{)}^{[13]} \quad (1)$$

where ω is the vibrational OH stretch frequency. It follows unequivocally that the higher the frequency of the O–H stretch mode the weaker the bonding between molecules (less pronounced binding of H atoms via intermolecular bonding).

More importantly, there is a correlation between hydrogen bond strength and intramolecular OH bond strength:^[14] following the bond conservation principle that states that the bonding capabilities of any atom is constant, the hydrogen bond with another molecule weakens the original OH-bond leading to a (positive) correlation between the frequency of the O–H stretch mode and the O–H bond strength (intramolecular bonding).^[14] Since the anharmonicity of the OH bond also decreases, the dissociation energy of the OH bond can decrease substantially due to the increasing strength of the hydrogen bonding.^[14] Considering this shows that the hypothesis of a causal relationship between the position of the O–H stretch and the potential at which oxygen evolution starts is justified. Therefore, the study of the O–H stretching vibration of aqueous solutions is scientifically warranted, to obtain a descriptor for the susceptibility of the O–H bond to cleavage based on structural-molecular realities. A strengthening (or

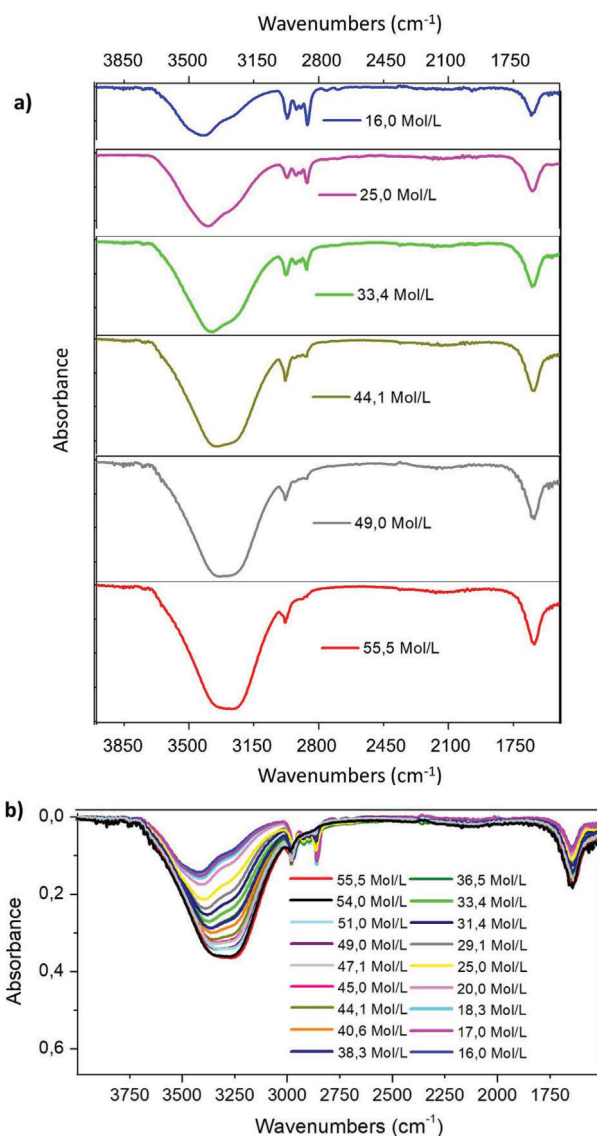


Figure 1. FTIR spectra of water/dioxane solutions. Absorbance vs wavenumbers plots. Selected spectra recorded with $c(\text{H}_2\text{O}) = 16; 25; 33.4; 44.1; 49$ and 55.5 mol L^{-1} (a). Overview of all recorded FTIR spectra.

weakening) of the O–H bond, intended to be cleaved during water electrolysis should therefore lead to a blue (red) shift in the O–H stretch mode. To our knowledge, the use of infrared spectroscopy for water-splitting applications has so far focused on the study of the solid–liquid interface to identify species and reaction mechanisms.^[15]

2. Results and Discussion

We recorded Fourier transform infrared (FTIR) spectra of dioxane/water solutions with concentration values of water (in dioxane) in between 16 and 55.5 mol L⁻¹ (pure pH 7 electrolyte) which corresponds to 0.66–1 mole fractions of water.

As we can take from **Figure 1a,b** the contour (3000–3700 cm⁻¹) is shifted with increasing (corresponding) dioxane content to

the high-frequency region (blueshift) and is partly split into discrete components most likely due to intramolecular stretch–stretch and intramolecular stretch–bend coupling. This shows that with increasing organic solvent content more separated water molecules (weakening of the hydrogen-bridge-based 3D molecular network) are now responsible for the absorption of radiation in the mentioned infrared region since pure dioxane shows no absorption above 3000 cm^{-1} . With decreasing dioxane content the contour is shifted to the low frequency (red-shift) region and the broadband is typical for hydrogen-bridged associated water molecules, that is, the fluctuation character of the 3D hydrogen network. This is nevertheless likely to be a direct reporter for the H–O bond strength in water molecules.^[14,16] Adding organic solvent results in a weakening of the interaction between water molecules and coincides with an increase in the O–H bond strength (intramolecular bonding).

In addition, one can derive from the plotted FTIR spectra that with increasing water content the intensity of the absorption that can be assigned to the stretching vibration increases, which is based on the increased amount of water relatively to the amount of dioxane. This effect overlaps with a stabilization effect that occurs in a narrow concentration range with its maximum at $\approx 37.8\text{ mol L}^{-1}$ which is also known to increase the OH oscillator stretching vibration band.^[17] At a certain, yet undetermined composition of dioxane/water mixture additional hydrogen bridges between the water molecules occur as a result of the interaction of water molecules with the dioxane molecules.

The O–H stretch frequency is known to be an excellent descriptor of the local hydrogen bonding arrangement in neat water. However, if other molecular species, especially those with O–H groups are present in the sample intermolecular interactions can arise. In the case of water/alcohol mixtures for instance intermolecular stretch–stretch coupling may occur.^[11] In addition to energy splitting between O–H stretch modes Fermi resonance with bending overtone can potentially complicate the interpretation of O–H stretch mode spectra. A common experimental approach to simplify the O–H stretch spectrum, based on a strong reduction of intramolecular stretch–stretch-, and intermolecular stretch–bend couplings utilizes liquid-isotope-diluted 5% HOD in D_2O . Here OD and OH stretches are largely decoupled and HOD molecules are surrounded by D_2O leading to a suppression of intermolecular vibrational couplings.^[18] However, since the bending mode is sensitive to hydrogen bonding, but not obscured by intermolecular vibrational coupling effects, the H–O–H bending mode spectra should not be ignored. We checked the bending mode derived from the FTIR spectroscopy experiment and, like the stretching mode data, detected a blueshift of the corresponding absorption band positioned at ≈ 1640 reciprocal wavelengths with increasing dioxane contents (Figure 2).

It is known that when dissolved in 1,4-dioxane, water molecules can, depending on the thermodynamic activity of water either exist as single molecules forming complexes with the organic solvent at very low water content (0–0.2 mole fractions of water) or as associated (H-bonded) molecules^[10] (at higher water content (>0.3 mole fractions of water)). In the region between 0.3 and 1 mole fractions of water, we either have microlayering which is based on the formation of water globules with a gapless network of hydrogen-bonded water molecules (0.3–0.8 mole fractions of water), or have undisturbed microstructure of water

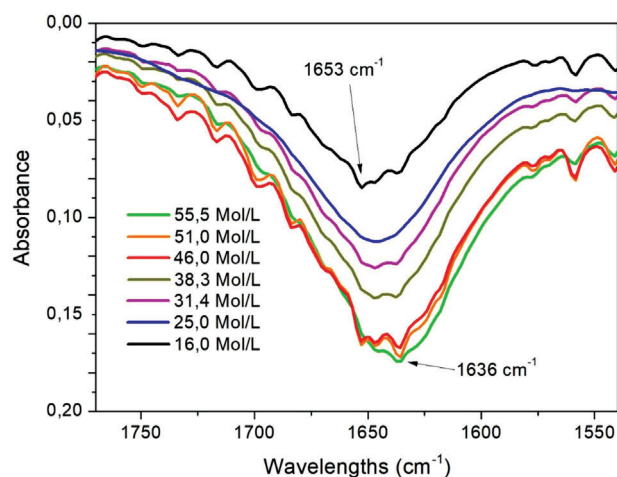


Figure 2. The H–O–H bending mode spectra of water/dioxane solutions. Absorbance vs wavenumbers plots.

(0.8–1 mole fractions of water).^[19] In our experiments, the water concentration of the water/dioxane solutions ranges between 16 and 55.5 mol L^{-1} which corresponds to 0.66–1 mole fractions of water.

With a minimal molarity of 16 mol water per liter solution, which corresponds to 0.66 mole fractions of water the isosbestic point due to the formation of 1:2 water/dioxane complexes is not reached.

Using a three-electrode setup consisting of a Pt working electrode (WE) (see Experimental Section) as an anode, a Pt counter electrode (CE), and an Ag/AgCl electrode as reference electrode (RE) we conducted cyclic voltammetry measurements upon exploitation of those previously used water/dioxane solutions (Figure 3).

A comparison of the individual cyclic voltammetry (CV) measurements recorded for different water/dioxane compositions shows the influence of the molecular structural conditions of the H_2O molecule on the onset potential. This is only correct and reliable if the influence of the working electrode on the onset potential of the oxygen evolution is the same for each CV measurement carried out. This, in turn, is only guaranteed if the electrode, so the electrocatalyst on the periphery of the electrode, is not subject to any changes whilst carrying out the CV experiments. To enable a reliable and reproducible determination of the potential at which the oxygen formation starts, the cyclic voltammetric investigations, therefore, had to be carried out very carefully and according to a strict protocol (see Experimental Section). To achieve, reproducible, reliable results for every CV-based determination of the OER onset potential, the OER electrocatalyst has to be freshly generated on the bare Pt metal and then removed again before the next measurement. Therefore, the Pt working electrode and the Pt counter electrode were cleaned in 10% HCl upon ultrasonication before starting the next CV measurement. The Pt working electrode was activated in a way that a new Pt-oxide layer was created on the surface. This was done using it as an anode for OER in a pH 7-corrected mixture of a $0.1\text{ M K}_2\text{HPO}_4/\text{KH}_2\text{PO}_4$ buffer solution. Prior to each CV test, zero current conditions at OER equilibrium potential need to be ensured to enable standardized conditions when using this

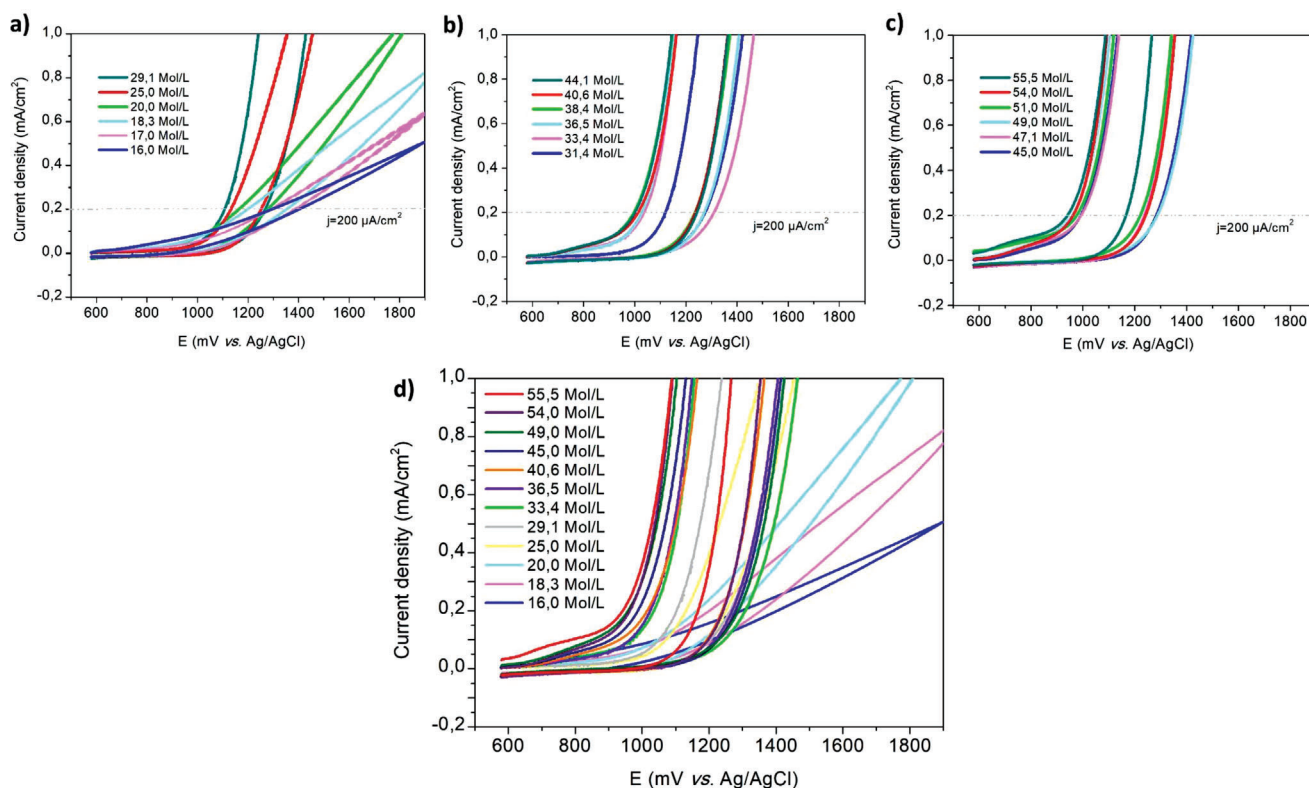


Figure 3. a–d) The results of cyclic voltammetry experiments performed with water/dioxane mixtures: 16.0–29.1 mol L⁻¹ H₂O (a); 31.4–44.1 mol L⁻¹ H₂O (b); 45.0–55.6 mol L⁻¹ H₂O (c), 16.0–55.5 mol L⁻¹ (d). Anode: electro-activated Pt; electrode area: 1 cm²; scan rate: 10 mV s⁻¹.

activated Pt anode in the desired dioxane/water mixture. This is realized through chronoamperometry experiments carried out in the dioxane/water mixture that is intended to be evaluated. A detailed description of the experimental protocol is given in the experimental part. Pure 1,4-dioxane showed no signs of electrochemical reactions when the potential of the working electrode was varied between 1.2 V vs reversible hydrogen electrode (RHE) and 2 V vs RHE, as confirmed by the electrochemical experiments (Figure S1, Supporting Information).

The CV curves recorded shifted with increasing dioxane content of the corresponding electrolyte to higher potentials. This shows that the potential at which oxygen formation begins, (defined as the potential at which the current density of the CV curve exceeds 200 $\mu\text{A cm}^{-2}$) increases with increasing dioxane content (Table 1). Given the results from both FTIR (Figure 1: the blueshift in absorbance vs wavenumbers curves with increasing dioxane content of the corresponding electrolyte) and the electrochemical testing (Figure 3: CV curves are shifted to higher potentials with increasing dioxane content) we conclude a positive correlation between the O–H stretch frequency (as derived from FTIR plots, Figure 1) and the onset of the oxygen evolution as derived from the CV scans (see also Figure 4). During the recording of the CV's neither the electrode geometry, nor the stirring speed, the vessel, or one of the electrodes were changed. Thus, the prerequisites for constant OER onset potentials are given (except for identical electrolytes). As mentioned, the combination of a Pt WE and a Pt CE turned out to create ideal conditions for very high reproducibility of the OER onset measurements. We em-

phasize at this point, however, that the results obtained with Pt electrodes can also be verified when using a steel working electrode (X20CoCrWMo10-9 electro-oxidized see Experimental Section for details). The recorded CV curves shift to higher potentials with increasing dioxane content. Therefore, there is also a positive correlation between the O–H stretching frequency and the onset of oxygen evolution in this case. This can be taken from the supporting information (Table S1, Figures S2, S3, Supporting Information).

Since the electrochemical results (Figure 3) are acquired under electrochemical fields we checked whether applying a bias voltage during the acquisition of the FTIR spectra has any influence on the outcome of the FTIR experiments (Figures S4–S6, Supporting Information). The FTIR spectra recorded with water concentrations of 29.1 and 52 mol L⁻¹ with or without bias potential were identical (Figures S3 and S4, Supporting Information).

We are aware that there is generally a large dependence of the OER onset potential on a variety of factors, such as the type of electrode, the pretreatment of the electrode, the catalytically active species (electrocatalyst), the type of electrolyte, the concentration of the ingredients just to name a few. However, if all these points except the electrolyte are kept strictly constant during a series of electrochemical measurements, and a stepwise change in the concentration of the electrolyte entails a constant change in the OER onset potential and the O–H stretching frequency, this can be used as evidence for the causal dependence of the OER onset potential on the OH bond strength (Intramolecular bonding; see Experimental Section).

Table 1. The left column displays the molarity of the 1,4-dioxane/water solutions respectively of the pure pH 7 electrolyte. Column II displays the O–H stretch frequency measured at the point at which there is a maximum regarding the absorbance. Column III displays the first momentum of the O–H stretch vibration band. Column IV shows the onset potential in V vs Ag/AgCl defined as the potential E at which the current density exceeds $j = 200 \mu\text{A cm}^{-2}$.

Molarity [Mol L ⁻¹ H ₂ O]	O–H stretch frequency [cm ⁻¹] Maximum	O–H stretch frequency [cm ⁻¹] First Momentum	Onset potential for OER [E in V vs Ag/AgCl at $j = 200 \mu\text{A cm}^{-2}$]
16.0	3419.4	3391.0	1298
17	3421.3	3387.5	1286
18.3	3410	3384.5	1205
20.0	3404	3379.7	1.16
25	3398.1	3360.7	1.13
29.1	3386.9	3355.3	1107
31.4	3383	3350.4	1.13
33.4	3375.3	3345.3	1.03
36.5	3371.4	3340.3	1026
38.3	3365.6	3339.0	0998
40.6	3365.6	3335.6	1017
44.1	3354.1	3331.3	1.00
45	3346.1	3328.1	0991
47.1	3338.6	3327.9	0994
49	3336.4	3325.2	0.96
51	3317.1	3324.3	0979
54	3278.6	3323.7	0.96
55.6	3265.3	3320.6	0.94

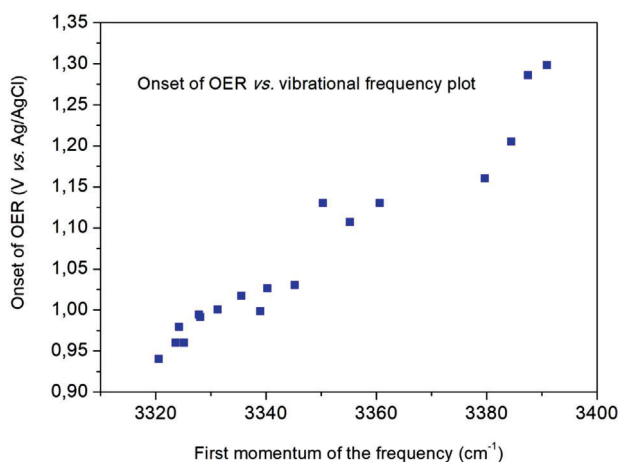


Figure 4. The positive correlation between the onset of oxygen evolution in V vs Ag/AgCl (as derived from cyclic voltammograms determined at $j = 200 \mu\text{A cm}^{-2}$) and the first momentum of the O–H stretch frequency (as determined from FTIR spectroscopic measurements).

3. Conclusion

The correlation between measured variables derived from simple physical measurements we used can be described as an adequate tool and is unexpected even for scientists who have studied the matter for years.

The O–H stretching frequency is a so far underestimated indicator of the readiness of water molecules to be split into their fission products.

With this new tool, scientists can study the influence of electrolytes on the OER onset potential, a key parameter of water electrolysis, and decouple it from various other influencing factors.

4. Experimental Section

The FTIR measurements were performed using a Bruker Vertex 70 FTIR spectrometer equipped with an ATR unit. The IR spectra were recorded at 2 cm^{-1} resolution in a spectral range from 400 to 4000 cm^{-1} . Two different setups were chosen for recording FTIR spectra when a bias potential of 1.65 V was simultaneously applied. A glass cuvette (Figure S4a,b, Supporting Information) equipped with 2 Pt electrodes was used. The ATR system was equipped with two Pt wire electrodes (Figure S4c, Supporting Information). A standard-size dry battery (AA battery) which delivered a quiescent terminal voltage of 1.65 V was exploited as the power source.

The computing of the first momentum of the frequency: For each concentration, two location parameters were computed by the maximum of the transmittance $f(x)$ and by its first normalized moment $\int_{\Omega} x f(x) dx / \int_{\Omega} f(x) dx$ where it was restricted to the field of view $\Omega = (3020, 3700)$, respectively.

Electrochemical Measurements Based on Pt WE and Pt CE: A three-electrode set-up was used for all electrochemical measurements. The Pt WE was made of Pt wire (Evochem Advanced Materials GmbH, Offenbach am Main, Germany), 0.5 mm in diameter, 60 cm in length which corresponded to an electrode area of 1 cm^2 .

A Pt wire (Evochem Advanced Materials GmbH, Offenbach am Main, Germany) electrode ($4 \times 5 \text{ cm}$ geometric area) was exploited as counter electrode and a silver–silver chloride (Ag/AgCl) electrode (Deutsche Metrohm GmbH & Co. KG; Kaninenberghöhe 8, 45136 Essen, Germany) with $c = 3 \text{ mol L}^{-1}$ KCl serving as reference electrode; therefore all voltages were quoted against this RE. The equilibrium potential of the OER amounted to 1.229 V vs normal hydrogen electrode (NHE) at pH 0 at standard pressure and at 298.15 K. According to the Nernst equation it amounted to +0.814 V vs NHE at pH 7. Given the activity constant of $f = 0.6$ ($c = 3 \text{ mol KCl L}^{-1}$) and $\phi_0(\text{Ag/AgCl}) = +0.207$ vs NHE at 298.15 K, the equilibrium potential of the OER amounted to +0.607 V vs Ag/AgCl at pH 7.

The voltammogram of pure 1,4-dioxane (Figure S1, Supporting Information) was recorded upon the exploitation of an RHE (HydroFlex, Gaskatel Gesellschaft für Gassysteme durch Katalyse und Elektrochemie mbH. D-34127 Kassel, Germany).

For all measurements, the RE was placed between the WE and the CE. The measurements were performed in a pH 7 corrected 0.1 M $\text{KH}_2\text{PO}_4/\text{K}_2\text{HPO}_4$ or in dioxane/pH 7 corrected 0.1 M $\text{KH}_2\text{PO}_4/\text{K}_2\text{HPO}_4$ solutions with a molarity of water in the range 16–55.5 mol L^{-1} . The pH 7 corrected 0.1 M $\text{KH}_2\text{PO}_4/\text{K}_2\text{HPO}_4$ solution was prepared as follows: aqueous solutions of 0.1 M K_2HPO_4 and KH_2PO_4 (VWR, Darmstadt, Germany) were mixed until the resulting solution reached a pH value of 7.0. 1,4-Dioxane (CAS 123-91-1) with a purity of >99% was purchased from Fisher Scientific, Japan.

The distance between the WE and the RE was adjusted to 1 mm and the distance between the RE and the CE was adjusted to 4–5 mm. All electrochemical data were recorded digitally using either a Potentiostat Keithley Tektronix 2460 SourceMeter, an Interface 1000 from Gamry Instruments (Warminster, PA 18 974, USA) or a Metrohm Autolab PGStat 20 (Ecochemie BV Utrecht, The Netherlands).

The three different potentiates were used in order to determine the reproducibility of determining the potential at which oxygen evolution begins.

Cyclic voltammograms (CV) were recorded in 80 mL of electrolyte in a 150 mL glass beaker under stirring (180 r min^{-1}) using a magnetic stirrer (15 mm stirring bar). The scan rate was set to 10 mV s^{-1} (Figure S1, Supporting Information: 20 mV s^{-1}) and the step size was 2 mV. The

potential was cyclically varied between +0.6 and +1.9 V vs Ag/AgCl. No IR compensation was performed whilst recording the CV plots.

Cyclic voltammetry measurements were carried out according to the following protocol: I) The counter electrode (Pt) and the working electrode (Pt) were cleaned upon ultrasonication in HCl (10% per weight) for 15 min at room temperature. II) The electrodes were rinsed in distilled water for 2 min. III) Both electrodes were treated in distilled water in an ultrasonic bath for 10 min. IV) A chronopotentiometry experiment was carried out upon usage of the Pt CE and WE in 80 ml of pH 7 corrected 0.1 M $\text{KH}_2\text{PO}_4/\text{K}_2\text{HPO}_4$ at a current density of 20 mA cm^{-2} for 1000 s. V) the pH 7 electrolyte was replaced with 80 mL of the electrolyte to be measured (water dioxane mixtures see Figure 3). VI) A chronoamperometry experiment was carried out at $E = 0.6 \text{ V}$ vs Ag/AgCl for 1000 s. VII) The actual CV measurement was performed. The potential of the WE was then kept constant at $E = 0.58 \text{ V}$ vs Ag/AgCl for 200 s before the start of the CV scan. Before the potential was dynamically changed, the device must ensure that the current density did not exceed $20 \mu\text{A cm}^{-2}$ (set equilibrium time to 100 s; stop equilibration at threshold $20 \mu\text{A}$). This procedure (Steps I–VII) was repeated after each CV experiment (i.e., after each measurement carried out with a specific water/dioxane mixture) to minimize any change in the working electrode during the performance of a CV sweep.

X20CoCrWMo10-9. As a modification to the protocol described above a steel working electrode constructed from stainless steel (SS) X20CoCrWMo10-9 (WST Werkzeug Stahl Center GmbH & Co. KG, D-90587 Veitsbronn-Siegelsdorf, Germany) with a total geometry of $70 \times 10 \times 1.5 \text{ mm}$ was used. An apparent surface area of 1 cm^2 was defined by an insulating tape. The SS was electroactivated prior to its usage as an anode as described in one of the previous reports^[20] (sample Co-300). Cyclic voltammetry measurements were carried out with dioxane/phosphate buffer solution mixtures as described above. The measurements were performed in a pH 7 corrected 0.1 M $\text{KH}_2\text{PO}_4/\text{K}_2\text{HPO}_4$ in dioxane/pH 7 corrected 0.1 M $\text{KH}_2\text{PO}_4/\text{K}_2\text{HPO}_4$ solutions with a molarity of water in the range 29.1–53.0 mol L^{-1} . The CVs were recorded in order of increasing dioxane content (starting with $c = 53.0 \text{ mol H}_2\text{O L}^{-1}$). The electrodes were not treated in any way between measurements. The potential of the WE was then kept constant at $E = 0.58 \text{ V}$ vs Ag/AgCl for 60 s before the start of the CV scan. Before the potential was dynamically changed, the device must ensure that the current density did not exceed $20 \mu\text{A cm}^{-2}$ (set equilibrium time to 30 s; stop equilibration at threshold $20 \mu\text{A}$). All electrochemical data were recorded digitally using Metrohm Autolab PGStat 20 (Ecochemie BV Utrecht, The Netherlands).

Supporting Information

Supporting Information is available from the Wiley Online Library or from the author.

Acknowledgements

The author would like to thank Prof. Dr. Mischa Bonn, MPI-P Mainz Germany, for the fruitful and helpful discussion of the manuscript (see also text written by him, i.e., Ref. [14]). In addition, the author thanks Anja Schuster for carrying out FTIR experiments.

Open access funding enabled and organized by Projekt DEAL.

Conflict of Interest

The authors declare no conflict of interest.

Data Availability Statement

The data that support the findings of this study are available from the corresponding author upon reasonable request.

Keywords

electrocatalysis, heterogeneous catalysis, renewable energy, water electrolysis

Received: January 4, 2023

Revised: April 17, 2023

Published online:

- [1] M. Chatenet, B. G. Pollet, D. R. Dekel, F. Dionigi, J. Deseure, P. Millet, R. D. Braatz, M. Z. Bazant, M. Eikerling, I. Staffell, P. Balcombe, Y. Shao-Horn, H. Schäfer, *Chem. Soc. Rev.* **2022**, *51*, 4583.
- [2] C. Wei, Z. Feng, G. G. Scherer, J. Barber, Y. Shao-Horn, Z. J. Xu, *Adv. Mater.* **2017**, *29*, 1606800.
- [3] H. Schäfer, M. Chatenet, *ACS Energy Lett.* **2018**, *3*, 574.
- [4] L. Trotochaud, S. L. Young, J. K. Ranney, S. W. Boettcher, *J. Am. Chem. Soc.* **2014**, *136*, 6744.
- [5] H. J. Bakker, J. L. Skinner, *Chem. Rev.* **2010**, *110*, 1498.
- [6] K. J. Tielrooij, N. Garcia-Araez, M. Bonn, H. J. Bakker, *Science* **2010**, *328*, 1006.
- [7] P. Ball, *Life's Matrix: A Biography of Water*, University of California Press, Berkeley, CA, USA **2001**.
- [8] D. S. Eisenberg, W. Kauzmann, *The Structure and Properties of Water*, Oxford University Press, New York **1969**.
- [9] Y. R. Shen, V. Ostroverkhov, *Chem. Rev.* **2006**, *106*, 1140.
- [10] V. A. Sirotkin, B. N. Solomonov, D. A. Faizullin, V. D. Fedotov, *J. Struct. Chem.* **2000**, *41*, 997.
- [11] T. Seki, K.-Y. Chiang, C.-C. Yu, X. Yu, M. Okuno, J. Hunger, Y. Nagata, M. Bonn, *J. Phys. Chem. Lett.* **2020**, *11*, 8459.
- [12] R. Rey, K. B. Møller, J. T. Hynes, *J. Phys. Chem. A* **2002**, *106*, 11993.
- [13] D. Ojha, K. Karhan, T. D. Kühne, *Sci. Rep.* **2018**, *8*, 16888.
- [14] Taken from personal correspondence with Professor Mischa Bonn, Max Planck Institute for Polymer Research, Department of Molecular Spectroscopy, Ackermannweg 10 55128 Mainz, Germany; January 03, 2023 11:42 CET.
- [15] A. Bieberle-Hütter, A. C. Bronneberg, K. George, M. C. M. van den Sanden, *J. Phys. D: Appl. Phys.* **2021**, *54*, 133001.
- [16] Y. A. Efimov, Y. A. Naberukhin, *Mol. Phys.* **1975**, *30*, 1621.
- [17] G. C. Pimentel, A. L. McClellan, *The Hydrogen Bond*, (Ed.: L. Pauling), Freeman, San Francisco, CA, USA **1960**, p. 200.
- [18] F. Perakis, L. De Marco, A. Shalit, F. Tang, Z. R. Kann, T. D. Kühne, R. Torre, M. Bonn, Y. Nagata, *Chem. Rev.* **2016**, *116*, 7590.
- [19] D. N. Glew, H. D. Mak, N. S. Rath, in *Hydrogen Bonded Solvent Systems*, (Ed.: A. K. Covington, P. Jones), Taylor and Francis, London, UK, **1968**.
- [20] H. Schäfer, D. M. Chevrier, K. Kuepper, P. Zhang, J. Wollschlaeger, D. Daum, M. Steinhart, C. Heß, U. Krupp, K. Müller-Buschbaum, J. Stangl, M. Schmidt, *Energy Environ. Sci.* **2016**, *9*, 2609.